Confined Wakes: A Numerical Solution of the Navier-Stokes Equations

JEAN PARIS and STEPHEN WHITAKER

Northwestern University, Evanston, Illinois

A numerical solution of the two-dimensional Navier-Stokes equations is presented for the confined wake formed by the merging of two-plane Poiseuille flow streams. The system of finite-difference equations for the stream function and vorticity is solved by the Peaceman-Rachford elimination method for Reynolds numbers of 1, 50, 387, and 647. While the stability of the numerical method is not a problem for this range of Reynolds numbers, the number of points in the finite-difference network (and hence the computation time) does become burdensome.

At high Reynolds numbers, the primary boundary-layer simplification is imposed to yield a set of parabolic equations for the vorticity and stream function. These equations are solved by a straightforward "marching" technique, thus providing a solution with a minimum of computational effort. The "boundary-layer equations" presented in this paper are not subject to the order of magnitude analysis which leads to the neglect of one of the momentum equations in order to obtain the Prandtl boundary-layer equations. The method outlined here represents an approximate solution for high Reynolds numbers, which gives surprisingly good agreement with the complete solution.

Often the equations of motion must be solved for conditions which cannot be treated by standard analytic methods. In general this situation occurs when the Reynolds number is large enough so that creep flow analysis is not valid, yet small enough so that boundary-layer methods cannot be applied. Nonhomogeneous boundary conditions and free surface flows may also represent problems which cannot be solved analytically. High Reynolds number flows, for which the boundary-layer assumptions may be valid, but for which no similarity transform exists (*6, 7, 12*), represent an area where numerical methods must be used.

Several approximate methods are available for solving the Navier-Stokes equations. The variational method recently proposed by Slattery (*17*) has been applied successfully to the problem of flow past a sphere (*5*) for Reynolds numbers up to 100. The Galerkin method (*9, 19, 20*) has proved useful also in studying this same problem and others. These two methods have the advantage that a functional representation of the flow field is obtained; however, the algebraic effort is immense. Numerical solutions of the equations of motion for flow past a cylinder have been obtained by means of relaxation techniques (*1*) and by the "squares" method proposed by Thom (*21*), and have been discussed in detail by Thom and Apelt (*22*). The relaxation method has been used by Wang and Longwell (*24*) to determine the flow field in the entrance region between parallel plates. Fromm and Harlow (*29*) have applied a technique resembling that described by Thom and Apelt to transient flows, and have successfully predicted the vortex shedding phenomena which occur in the wake of a flat plate placed perpendicular to the flow. Pearson (*30*) has commented extensively on the choice of numerical methods for solving the time-dependent problem, and concludes that relaxation types of iteration methods are satisfactory when the nonlinear terms are small, but that the Peaceman-Rachford (*31*) implicit alternating direction method is superior when the nonlinear terms are large. In this study the line-by-line matrix inversion suggested by Thomas (*23*) and first applied by Peaceman et al. (*15*) was successfully used to determine both the stream function and vorticity for Reynolds numbers up to 647.

Jean Paris is with Procter and Gamble Company, Cincinnati, Ohio, and Stephen Whitaker is with the University of California, Davis, California.

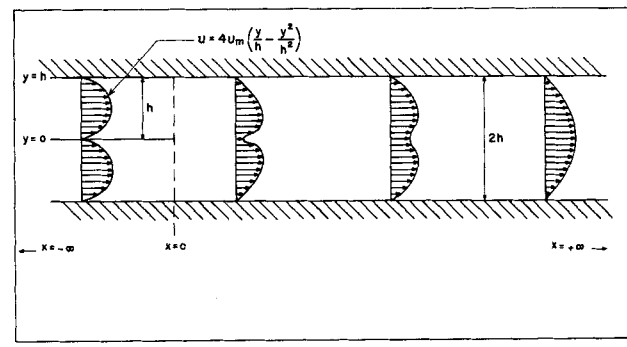

Fig. 1. Flow configuration.

Formulation of the Navier-Stokes equations in terms of the stream function and vorticity yields a stable system of finite-difference equations. The problem may also be formulated in terms of a single fourth-order equation for the stream function; however, previous experience (*2*) with this form of the equations indicated that boundary conditions associated with the fourth-order equation present serious difficulties. Pearson (*30*) has compared the two approaches and found that an order of magnitude more computer time was required to solve the single equation than was required to solve the two second-order equations.

DISCUSSION

The flow configuration under consideration is illustrated in Figure 1. It consists of two plane Poiseuille flow streams, separated by an infinitely thin plate, which merge at $x = 0$ to form a single plane Poiseuille flow stream at $x \to \infty$. For steady, two-dimensional, incompressible, isothermal flow of a Newtonian fluid, the equations of motion are

$$u\frac{\partial u}{\partial x} + v\frac{\partial u}{\partial y} = -\frac{1}{\rho}\frac{\partial p}{\partial x} + \nu\left(\frac{\partial^2 u}{\partial x^2} + \frac{\partial^2 u}{\partial y^2}\right) \quad (1)$$

$$u\frac{\partial v}{\partial x}+v\frac{\partial v}{\partial y}=-\frac{1}{\rho}\frac{\partial p}{\partial y}+\nu\left(\frac{\partial^2 v}{\partial x^2}+\frac{\partial^2 v}{\partial y^2}\right) \quad (2)$$

and the continuity equation is

$$\frac{\partial u}{\partial x}+\frac{\partial v}{\partial y}=0 \quad (3)$$

If the dimensionless stream function ψ and dimensionless vorticity Ω are defined as

$$U=\frac{\partial \psi}{\partial Y},\ V=-\frac{\partial \psi}{\partial X},\ \text{and}\ \Omega=\frac{\partial U}{\partial Y}-\frac{\partial V}{\partial X}$$

where $U = u/u_m$
$V = v/u_m$
$X = x/h$
$Y = y/h$

Equations (1), (2), and (3) may be written as

$$\nabla^2\Omega=N_{Re}\left(\frac{\partial \psi}{\partial Y}\frac{\partial \Omega}{\partial X}-\frac{\partial \psi}{\partial X}\frac{\partial \Omega}{\partial Y}\right) \quad (4)$$

$$\nabla^2\psi=\Omega \quad (5)$$

where

$$\nabla^2=\frac{\partial^2}{\partial X^2}+\frac{\partial^2}{\partial Y^2}$$
$N_{Re} = u_m h/\nu$
u_m = centerline velocity at $x = \infty$

Since the flow is symmetric about $y = 0$, only the region, $0 \leq y \leq h$, need be considered. The boundary conditions are

$$\text{B.C. 1}\quad \frac{\partial u}{\partial x}=0;\ x\to\pm\infty \quad (6)$$

$$\text{B.C. 2}\quad u=v=0;\ y=h \quad (7)$$

$$\text{B.C. 3}\quad u=v=0;\ y=0,\ x\leq 0 \quad (8)$$

$$\text{B.C. 4}\quad \frac{\partial u}{\partial y}=v=0;\ y=0,\ x>0 \quad (9)$$

The boundary conditions at $x \to \pm \infty$ need to be considered further. In general, one would be inclined to specify the parabolic velocity profile for $x \to \pm \infty$; however, a boundary condition should be based on physical considerations without the aid of the differential equations. The use of the parabolic profile as a boundary condition is equivalent to imposing B.C. 1 on the continuity equation to determine that $v = 0$ for $x \to \pm \infty$, and then solving Equations (1) and (2) for the velocity distribution. While we often use the limiting solution of a differential equation as a boundary condition, it will be beneficial not to do so in this case. In terms of ψ and Ω the boundary conditions become

$$\text{B.C. 1}a\quad \frac{\partial \psi}{\partial X}=\frac{\partial \Omega}{\partial X}=0;\ X\to\pm\infty \quad (10)$$

$$\text{B.C. 2}a\quad \psi=2/3,\frac{\partial \psi}{\partial Y}=0;\ Y=1 \quad (11)$$

$$\text{B.C. 3}a\quad \psi=\frac{\partial \psi}{\partial Y}=0;\ Y=0,\ X\leq 0 \quad (12)$$

$$\text{B.C. 4}a\quad \psi=\Omega=0;\ Y=0,\ X>0 \quad (13)$$

Of particular importance here is that neither Ω nor derivatives of Ω are specified on the solid boundaries. For elliptic equations such as Equations (4) and (5), it is well known that a unique solution is obtained only when the function or derivatives of the function normal to the boundary are known everywhere on the boundary. This is not the case for the vorticity equation; however, we are dealing with a set of coupled, partial differential equations, and the usual conditions for uniqueness do not apply. Before going into the details of the vorticity condition of the solid boundaries and the treatment of the conditions at infinity, the method of solution will be described.

NUMERICAL SOLUTION

The finite-difference forms of Equations (4) and (5) are obtained by representing the first and second derivatives by the standard formulas

$$\left(\frac{\partial f}{\partial x}\right)=(f_{n+1}-f_{n-1})/2\Delta x$$

$$\left(\frac{\partial^2 f}{\partial x^2}\right)=(f_{n+1}-2f_n+f_{n-1})/\Delta x^2$$

With n and j as the running indices in the X and Y directions, respectively, the finite-difference forms of the vorticity and stream function equations may be written for every interior point in the network illustrated in Figure 2. Equation (4) becomes

$$\Omega_{n-1,j}-2\left(1+\frac{\Delta X^2}{\Delta Y^2}\right)\Omega_{n,j}+\Omega_{n+1,j}=D_{n,j} \quad (14)$$

where

$$D_{n,j}=-\frac{\Delta X^2}{\Delta Y^2}(\widetilde{\Omega}_{n,j+1}+\widetilde{\Omega}_{n,j-1})+\frac{N_{Re}}{4}\left(\frac{\Delta X}{\Delta Y}\right)[(\widetilde{\psi}_{n,j+1}-\widetilde{\psi}_{n,j-1})(\widetilde{\Omega}_{n+1,j}-\widetilde{\Omega}_{n-1,j})-(\widetilde{\psi}_{n+1,j}-\widetilde{\psi}_{n-1,j})(\widetilde{\Omega}_{n,j+1}-\widetilde{\Omega}_{n,j-1})] \quad (15)$$

and Equation (5) may be written as

$$\psi_{n,j-1}-2\left(1+\frac{\Delta Y^2}{\Delta X^2}\right)\psi_{n,j}+\psi_{n,j+1}=E_{n,j} \quad (16)$$

where

$$E_{n,j}=\Delta Y^2\widetilde{\Omega}_{n,j}-\frac{\Delta Y^2}{\Delta X^2}(\widetilde{\psi}_{n+1,j}+\widetilde{\psi}_{n-1,j}) \quad (17)$$

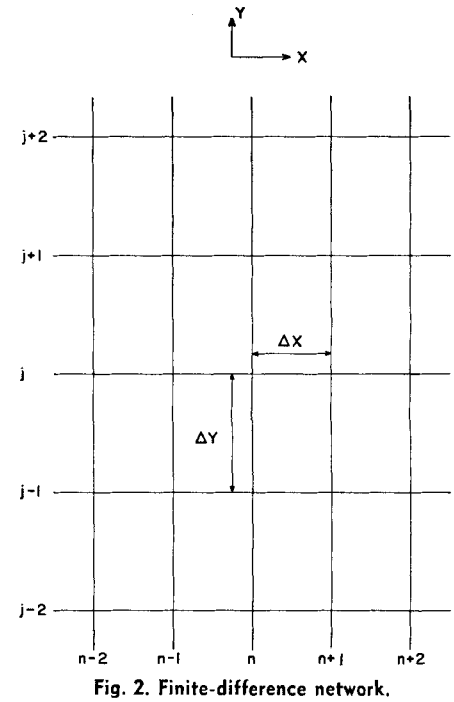

Fig. 2. Finite-difference network.

The terms marked by a tilde ($\sim$) represent assumed values based on a previous calculation. In this respect $D_{n,j}$ and $E_{n,j}$ are known quantities. Notice that $\Omega_{n+1,j}$ and $\Omega_{n-1,j}$ appear in the term $D_{n,j}$ as assumed values, yet they are also present as unknowns on the left-hand side of Equation (14). It would seem reasonable to include as many of the unknown terms as possible on the left-hand side of Equation (14); however, the computer program is considerably easier to write, and the computation time for each iteration is significantly shortened if these two terms are included in $D_{n,j}$. Of more importance is the fact that the iterative procedure appears to diverge (*14*) if the terms in question are included in the left-hand side of Equation (14).

In essence, Equations (4) and (5) are arranged in the form

$$\frac{\partial^2 \Omega}{\partial X^2} = f(X, Y) \tag{18}$$

$$\frac{\partial^2 \psi}{\partial Y^2} = g(X, Y) \tag{19}$$

which, for any given iteration, take the form of ordinary, second-order, nonhomogeneous differential equations which are easily solved at each value of $Y_j = j\Delta Y$ and $X_n = n\Delta X$, respectively. For any given problem, the choice of the form into which Equations (4) and (5) should be cast depends on the boundary conditions and the whims of the investigator. Since the boundary values of Ω had to be calculated at $Y = 0, 1$ for all X it was necessary to put the vorticity equation in the form of Equation (18). The stream function equation was formulated as Equation (19) because it appeared intuitively that the iterative procedure would be more stable if the line-by-line matrix inversion of this equation were carried out in the direction perpendicular to the vorticity equation. This approach is suggested by the success of the alternating direction method for solving the diffusion equation (28); however, in principle, the system of equations could as easily be solved if the stream function equation were arranged in the form

$$\frac{\partial^2 \psi}{\partial X^2} = G(X, Y) \tag{20}$$

Writing Equation (14) for each point on a line of constant j yields $N - 2$ equations, where N is the number of points in the X direction. If the slope is given on the boundaries [B.C. 1*a*, Equation (10)], there will be $N - 2$ unknowns associated with the $N - 2$ equations, which may be arranged in matrix form

$$\begin{bmatrix} C & 1 & & & & & \\ 1 & C & 1 & & & & \\ & 1 & C & 1 & & & \\ & & & 1 & C & 1 & \\ & & & & 1 & C & 1 \\ & & & & & 1 & C \end{bmatrix} \begin{bmatrix} \Omega_{1,j} \\ \Omega_{2,j} \\ \\ \\ \Omega_{N-2,j} \\ \Omega_{N-1,j} \end{bmatrix} = \begin{bmatrix} D_{1,j} \\ D_{2,j} \\ \\ \\ D_{N-2,j} \\ D_{N-1,j} \end{bmatrix}; j = 1, 2, \ldots J-1 \tag{21}$$

where

$$C = -2\left(1 + \frac{\Delta X^2}{\Delta Y^2}\right)$$

Equation (21) may be more conveniently written as

$$[\mathbf{C}]\,\Omega_j = \mathbf{D}_j;\ j = 1,2, \ldots . J-1 \tag{22}$$

where $[\mathbf{C}]$ is a tridiagonal matrix of coefficients and Ω_j and $\mathbf{D}_j$ are column vectors. A similar set of matrix equations may be written for the stream function

$$[\mathbf{C}']\,\psi_n = \mathbf{E}_n;\ n = 1,2, \ldots . N-1 \tag{23}$$

where

$$C' = -2\left(1 + \frac{\Delta Y^2}{\Delta X^2}\right)$$

The boundary conditions are incorporated into the matrix equations, and a solution results for a single interation when line-by-line matrix inversion is carried out for Equations (22) and (23). Thus

$$\Omega_j = [\mathbf{C}]^{-1}\,\mathbf{D}_j;\ j = 1,2, \ldots . J-1 \tag{24}$$

$$\psi_n = [\mathbf{C}']^{-1}\,\mathbf{E}_n;\ n = 1,2, \ldots . N-1 \tag{25}$$

The method of matrix inversion is straightforward and is described elsewhere (*14, 15*).

Since the values of $D_{n,j}$ and $E_{n,j}$ are based on assumed values of $\Omega_{n,j}$ and $\psi_{n,j}$, the solution of Equations (22) and (23) must be repeated until the calculated and assumed values are essentially identical. The criterion for convergence must be intuitive rather than mathematical, for at the present time, there appears to be no theoretical criterion for determining the upper or lower bound for a sequence of calculated values unless the sequence is oscillatory. An intuitive measure of convergence often is taken as the relative error for each iteration

$$\text{relative error } (\psi) = \sum_{n,j} \left| \frac{\psi^k_{n,j} - \tilde{\psi}^k_{n,j}}{\tilde{\psi}^k_{n,j}} \right| \tag{26}$$

The question that must be answered if the relative error is to be used as a measure of convergence is: How is the relative error related to the absolute error? The latter is defined as

$$\text{absolute error } (\psi) = \sum_{n,j} \left| \frac{\psi^k_{n,j} - \psi^\infty_{n,j}}{\psi^\infty_{n,j}} \right| \tag{27}$$

where $\psi^\infty_{n,j}$ is the value of the stream function for $k \to \infty$. This is not the true value of the stream function as determined by the differential equations and boundary conditions, nor is it the exact solution of the finite-difference equations. Providing the numerical method is stable and converging, $\psi^x_{n,j}$ represents the solution of the finite-difference equations subject to roundoff error. The point which must be kept in mind when considering the question of convergence is that small values of $(\psi^k_{n,j} - \tilde{\psi}^k_{n,j})$ do not guarantee small values of $(\psi^k_{n,j} - \psi^x_{n,j})$, and the use of the relative error as a measure of convergence must fall under Birkhoff's (3) classification of a plausible intuitive hypothesis.

Since an intuitive criterion for convergence was necessary, it seemed appropriate to examine the velocity field to determine whether significant variations were taking place. It appears reasonable to assume that intuition is applied more soundly to the velocity field than the error associated with successive iterations. An illustration of the progressive changes in the velocity for Reynolds numbers of 1 and 647 is shown in Figure 3, where it is seen that a converged solution is obtained in two hundred fifty iterations for $N_{Re} = 1$ and one hundred fifty iterations for $N_{Re} = 647$.

In examining Figure 3 one must keep in mind that the abscissa is logarithmic, thus the flat portions of the curves for $N_{Re} = 647$ extend over nearly fifty iterations. While the curves for $N_{Re} = 1$ vary more rapidly with k, the dimensionless velocity at $X = 1.0$ and $Y = 0.0$ has reached a value of 0.98, which is within 2% of the maximum permissible value for the dimensionless velocity. Further computation could have led only to meager changes in

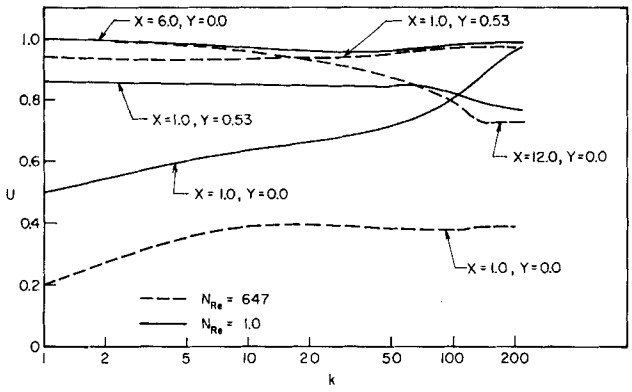

Fig. 3. Convergence of the velocity field.

the velocity field. Before discussing the results, it will be necessary to examine the finite-difference form of the boundary conditions in some detail.

BOUNDARY CONDITIONS

Equations (4) and (5) constitute a set of coupled, elliptic, partial differential equations. In general, a unique solution to an elliptic equation will exist if either the slope or the function is specified everywhere on the boundary. The stream function satisfies these conditions and, in addition, both the function and the slope are specified on the solid boundaries [B.C. 3*a*, Equation (12)]. In this respect, ψ would be overdetermined if Ω were given. In contrast to the stream function, the vorticity or its slope is specified everywhere except on the solid boundaries.

Previous investigators have made use of Equation (5) and the condition that ψ is a constant along a solid boundary to obtain the equation

$$\Omega = \frac{\partial^2 \psi}{\partial n^2}, \text{ at a solid boundary} \qquad (28)$$

where n = distance measured normal to the boundary which is used to calculate the vorticity and thus obtain a boundary value for the vorticity equation. However, Equation (5) and the boundary condition ψ equals a constant along a solid boundary, have been used to determine ψ and cannot be used again to determine Ω. Application of Equation (28) leaves the problem unspecified.

There appears to be two ways to treat the boundary conditions properly. The first requirement for ψ and Ω is that they satisfy Equations (4) and (5) everywhere within the region under consideration, and on the boundaries for this region. There is an infinity of solutions which satisfy this requirement; however, it can be shown (*13*) that a unique solution results for an elliptic equation when the function or its slope is specified everywhere on the boundary. Difficulty arises from the fact that the vorticity need only satisfy boundary conditions along some, not all, of the boundaries. However, there is another condition which Ω must satisfy; that is Ω must be a function such that the solution to Equation (5), which contains Ω as the nonhomogeneous part, will satisfy

$$\psi = \text{constant, on the solid boundaries} \qquad (29)$$

and

$$\frac{\partial \psi}{\partial n} = 0, \text{ on the solid boundaries} \qquad (30)$$

It is this latter condition which has not been satisfied by previous investigators, with the exception of Jenson (*8*). Jenson, in his study of flow past a sphere, fit the values of the stream function near the solid boundaries to a third-order polynomial subject to the restriction given by Equation (30). In this manner he obtained values of Ω and ψ which satisfied (approximately) the differential equations and all the boundary conditions. This appears to be a satisfactory technique and is used in the high Reynolds number solution; however, in this part of the analysis we chose simply to restrict ourselves to a method consistent with the condition that the equations must be satisfied everywhere within the region and on the boundaries. Thus when a boundary condition does not exist, one must solve the differential equation along the boundary. With this in mind we write Equation (22) as

$$[\mathbf{C}]\ \Omega_j = \mathbf{D}_j, j = 0,1,2, \ldots\ldots, J-1, J, X \leq 0 \qquad (31)$$

$$[\mathbf{C}]\ \Omega_j = \mathbf{D}_j, j = 1,2, \ldots\ldots, J-1, J, X > 0 \qquad (32)$$

Along the solid boundaries

$$\frac{\partial \psi}{\partial Y} = \frac{\partial \psi}{\partial X} = 0 \qquad (33)$$

and Equation (4) becomes

$$\nabla^2 \Omega = 0, \text{ on the solid boundaries} \qquad (34)$$

thus the matrix equations take a somewhat different form for $j = 0, J$. In obtaining the finite-difference form of Equation (34), $\left(\frac{\partial^2 \Omega}{\partial Y^2}\right)$ was written with $j = 1, J-1$ as the central points, whereas $\left(\frac{\partial^2 \Omega}{\partial X^2}\right)$ was written for $j = 0, J$; thus the two derivatives did not have the same central point. Higher order finite-difference equations could have been used to approximate $\left(\frac{\partial^2 \Omega}{\partial Y^2}\right)$ at Y = 0,1; however, this was not done since higher order equations often lead to instability (*18*).

The boundary conditions at $X \to \pm \infty$ obviously cannot be treated exactly with numerical methods. The conditions at $X \to -\infty$ present no serious difficulty, since it is well established (*11*) that the disturbance caused by the merging of two streams does not propagate but one- or two-channel depths upstream from the point $X = 0$. In this work the parabolic profile was assumed to exist at $X = -2$; thus the boundary conditions for ψ and Ω were taken to be

$$\text{B.C. } 1b \quad \psi = 4\left(\frac{Y^2}{2} - \frac{Y^3}{3}\right), \Omega = 4(1-2Y); X = -2 \qquad (35)$$

It would have been equally satisfactory to set the derivatives of ψ and Ω equal to zero as indicated by B.C. 1*a*;

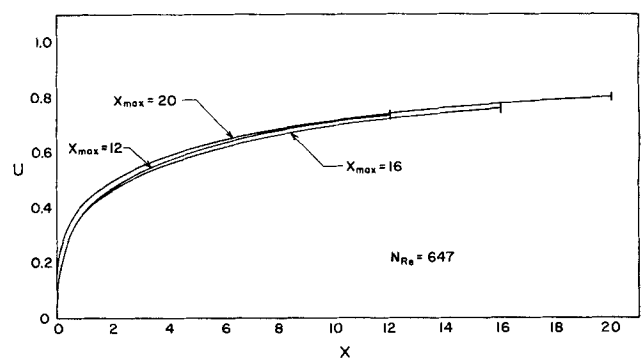

Fig. 4. Effect of downstream boundary condition on centerline velocity.

however, the use of the parabolic profile creates no difficulty at this point. This will not be the case with the downstream boundary conditions.

Presumably the parabolic profile could be specified at some distance far enough downstream so that it would become a satisfactory boundary condition. However, in practice, the computation time becomes excessive owing to the large number of points which must be used. This difficulty may be overcome by the use of a coordinate transformation of the type, $\eta = X/(1 + \beta X)$, which was used by Wang and Longwell (24), or by the use of variable mesh size (25). Both methods allow the downstream boundary condition to be placed far downstream without the use of an excessive number of mesh points; however, these techniques make programming more tedious and increase the computation time for a fixed number of points.

Because the equations of motion tend to be parabolic in nature when the Reynolds number is large, it appears that reasonable results may be obtained without the use of a coordinate transformation or a variable mesh size, unless one wishes definitely to determine the flow field far downstream. In this work, satisfactory results were obtained when the boundary conditions

$$\text{B.C. } 1c \quad \frac{\partial \psi}{\partial X} = \frac{\partial \Omega}{\partial X} = 0, X = X_{max} \tag{36}$$

were imposed where the velocity profile was quite different from parabolic. This fact is illustrated in Figures 4 and 5. Figure 4 shows the calculated centerline velocity for $N_{Re} = 647$ when the boundary conditions where imposed at $X_{max} = 12$, 16, and 20. These profiles are far from parabolic, as is seen in Figure 5, yet the velocity field is influenced only slightly as the position of the boundary is changed. There surely is some effect of the position of the downstream boundary condition, and if precise results are required, the coordinate transformation seems to be in order. However, the spread of the results is only 10%, and when limited computer time is available the boundary condition expressed by Equation (36) seems to be quite suitable.

The success of this approach may be explained as follows. Strictly speaking, the equations of motion are elliptic; however, at high Reynolds numbers derivatives with respect to X generally become negligible compared to derivatives with repect to Y, and the equations tend to become parabolic in nature. For truly parabolic equations a unique solution is obtained only for an open boundary in the positive X direction. This is not the case for the problem under consideration; however, the boundary condition expressed by Equation (36) is a "weak" condition, while the parabolic profile expressed by Equation (37)

$$\text{B.C. } 1d \quad \psi = Y - \frac{Y^3}{3}, \Omega = -2Y \tag{37}$$

represents a "strong" condition. As $N_{Re} \to \infty$ the equations of motion become more parabolic in nature, and the weak boundary condition plays an increasingly unimportant role in determining the solution. Thus it appears to be the most appropriate form of the downstream boundary condition for examining problems of this type. At low Reynolds numbers there is no difficulty in placing the boundary condition sufficiently far downstream, and identical results are obtained using either B.C. 1*c* or B.C. 1*d*.

DISCUSSION OF RESULTS

The calculated velocity profiles for $N_{Re} = 1$, 50, 387, and 647 are shown in Figures 6, 7, 8, and 9, respectively. For each Reynolds number, the number of iterations required for convergence (as determined by the behavior of the velocity field) was determined. These results, along with the maximum value of α are listed in Table 1. The iteration parameter α is used to predict the next assumed value of the stream function and vorticity on the basis of Equation (38).

$$\tilde{\psi}^{k+1}_{n,j} = \alpha \psi^{k}_{n,j} + (1 - \alpha) \tilde{\psi}^{k}_{n,j} \tag{38}$$

Values of α larger than the maximum value result in an unstable condition.

The steadily decreasing value of α with increasing Reynolds number is a clear indication that the system is less stable at the higher Reynolds numbers. Since the rate of convergence must go to zero as $\alpha \to 0$, it is surprising to see that the rate of convergence actually increases with Reynolds number. There may be two reasons why this is so. First, the criterion for convergence is rather qualitative and the results listed in Table 1 may be in error, although the curves shown in Figure 3 certainly indicate a more rapid rate of convergence at the higher Reynolds number. Second, the velocity profiles change markedly with Reynolds number and this may lead to differences in the rate of convergence. At low Reynolds numbers the velocity changes rapidly with X, thus large gradients of the vorticity and stream function are encountered and convergence is difficult. At high Reynolds numbers these large gradients are not present, and convergence is somewhat easier even though the system of equations becomes more nonlinear.

The mesh size ranged from

$$\Delta X = 0.25, \Delta Y = 0.05$$

for low Reynolds numbers, to

$$\Delta X = 0.5, \Delta Y = 0.05$$

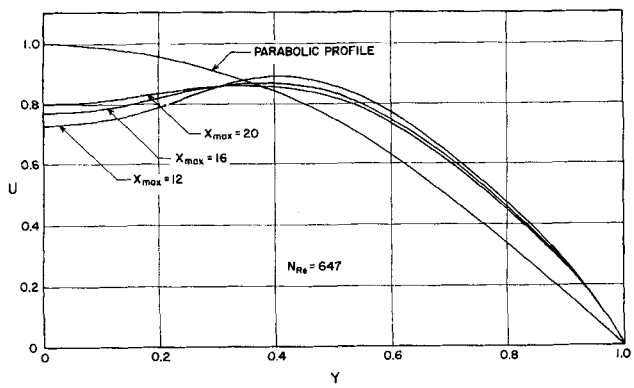

Fig. 5. Velocity profiles at downstream boundary.

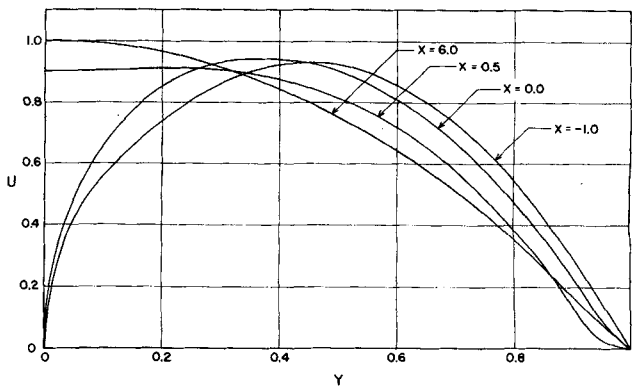

Fig. 6. Velocity profiles for $N_{Re} = 1$.

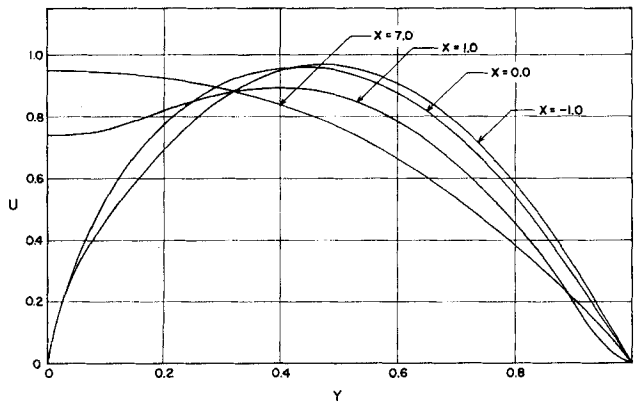

Fig. 7. Velocity profiles for $N_{Re} = 50$.

for the high Reynolds number. Since only limited computer time was available the mesh size was not changed to determine the error inherent in the finite-difference form of the equations. Fortunately, an estimate of the error may be obtained by comparison with a boundary-layer solution, and by examining the error of the macroscopic momentum balance. This will be discussed in the following section.

HIGH REYNOLDS NUMBERS

At high Reynolds numbers we might venture forth with the intuitive hypothesis that "variations of u in the x direction are small compared to variations of u in the y direction." This immediately leads to the inequalities

$$v << u, \frac{\partial u}{\partial x} << \frac{\partial u}{\partial y}, \frac{\partial^2 u}{\partial x^2} << \frac{\partial^2 u}{\partial y^2} \tag{39}$$

which we know are not valid at:

(1) the region near $x = 0$

(2) the two points in the channel at which $\dfrac{\partial u}{\partial y} = 0$

(3) the inflection point where $\dfrac{\partial^2 u}{\partial y^2} = 0$

While the assumptions indicated by Equation (39) are not valid at these three regions in the flow field, they would certainly appear to be satisfactory for most of the flow field. In terms of the stream function and the vorticity, the inequalities reduce to

$$\frac{\partial^2 \psi}{\partial X^2} << \frac{\partial^2 \psi}{\partial Y^2}, \frac{\partial^2 \Omega}{\partial X^2} << \frac{\partial^2 \Omega}{\partial Y^2} \tag{40}$$

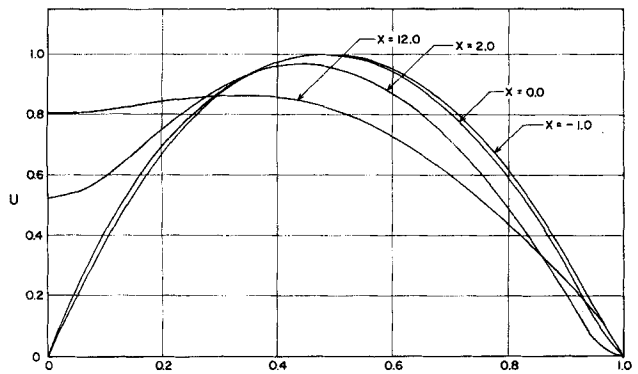

Fig. 8. Velocity profiles for $N_{Re} = 387$.

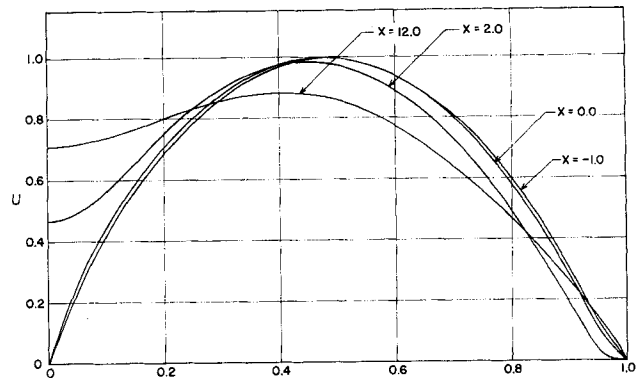

Fig. 9. Velocity profiles for $N_{Re} = 647$.

and Equations (4) and (5) become

$$\frac{\partial^2 \Omega}{\partial Y^2} = N_{Re}\left(\frac{\partial \psi}{\partial Y}\frac{\partial \Omega}{\partial X} - \frac{\partial \psi}{\partial X}\frac{\partial \Omega}{\partial Y}\right) \tag{41}$$

$$\frac{\partial^2 \psi}{\partial Y^2} = \Omega \tag{42}$$

It is of considerable importance to notice that Equations (41) and (42) may be obtained directly from Equations (43), (44), and (45).

$$U\frac{\partial U}{\partial X} + V\frac{\partial V}{\partial Y} = -\frac{\partial P}{\partial X} + \frac{1}{N_{Re}}\left(\frac{\partial^2 U}{\partial Y^2}\right) \tag{43}$$

$$U\frac{\partial V}{\partial X} + V\frac{\partial V}{\partial Y} = -\frac{\partial P}{\partial P} + \frac{1}{N_{Re}}\left(\frac{\partial^2 V}{\partial Y^2}\right) \tag{44}$$

$$\frac{\partial U}{\partial X} + \frac{\partial V}{\partial Y} = 0 \tag{45}$$

where

$$P = \frac{p}{\rho u_m^2}$$

by eliminating the dimensionless pressure P and using the definitions for ψ and Ω. Equations (43) and (45) readily result from the standard boundary-layer order of magnitude analysis (*16*) which indicates that

$$\frac{\partial^2 V}{\partial X^2} << \frac{\partial^2 V}{\partial Y^2}, \frac{\partial^2 U}{\partial X^2} << \frac{\partial^2 U}{\partial Y^2} \tag{46}$$

When one makes use of these inequalities the equations of motion are reduced from elliptic to parabolic equations. If "small causes $\left(\text{that is, the terms } \dfrac{\partial^2 V}{\partial X^2} \text{ and } \dfrac{\partial^2 U}{\partial X^2}\right)$ lead to small effects" this change in the nature of the equations may be of little importance. However, the inequality

$$V << U \tag{47}$$

is just as valid as those given by Equation (46); yet we cannot use this inequality to argue that all the terms in Equation (44) are negligible. This would lead us to the Prandtl boundary-layer equations which form an indeterminant set of two equations [(43) and (45)] and three unknowns (U, V, and P). In this case a small cause certainly does not lead to a small effect. Thus we find ourselves in the unenviable position of indulging in what might be called a "partial order of magnitude analysis." However previous work has indicated success in such endeavors and we are encouraged to continue.

To solve Equations (41) and (42) numerically, we first eliminate the Reynolds number as a parameter by

TABLE 1. EFFECT OF REYNOLDS NUMBER ON THE RATE OF CONVERGENCE

Reynolds number	1	50	387	647
Maximum α	0.6	0.4	0.2	0.2
Iterations required for convergence	250	250	200	150

writing

$$\frac{\partial^2\Omega}{\partial Y^2} = \left(\frac{\partial\psi}{\partial Y}\frac{\partial\Omega}{\partial\overline{X}} - \frac{\partial\psi}{\partial\overline{X}}\frac{\partial\Omega}{\partial Y}\right) \tag{48}$$

where

$$\overline{X} = X/N_{Re}$$

and write the finite-difference forms as indicated by Equations (49) and (50).

$$\Omega_{n+1,j-1} - 2\Omega_{n+1,j} + \Omega_{n+1,j+1} = \Delta Y^2\left(\frac{\partial\psi}{\partial Y}\frac{\partial\Omega}{\partial\overline{X}} - \frac{\partial\psi}{\partial\overline{X}}\frac{\partial\Omega}{\partial Y}\right)_{n+1/2,j} \tag{49}$$

$$\psi_{n+1,j-1} - 2\psi_{n+1,j} + \psi_{n+1,j+1} = \Delta Y^2\,\Omega_{n+1,j} \tag{50}$$

The conditions at $\overline{X} = 0$ are given by

$$\Omega = 4(1-2Y), \psi = 4\left(\frac{Y^2}{2} - \frac{Y^3}{3}\right)$$

One need only assume values of ψ and Ω for $\overline{X} = \Delta\overline{X}$ in order to obtain new calculated values of ψ and Ω by means of Equations (49) and (50). The next set of assumed values is determined by means of Equation (38), and the calculation is repeated. When the difference between the assumed values and the calculated values is negligible, a new step in the $\overline{X}$ direction is taken and the iterative process repeated.

Values of ΔY were the same as those used in the previous solution; however, ΔX was doubled for each step to reduce computation time. There was considerable difficulty in obtaining a converged solution for the first few steps. When $\overline{X} = \Delta\overline{X} = 0.00025$ the iteration parameter α had to be less than 0.004, and four thousand iterations were required for convergence. However, the maximum value of α could be rapidly increased as $\Delta\overline{X}$ became larger and only seven thousand iterations were required to obtain converged values for the nine values of $\overline{X}$ used to describe the velocity field between $\overline{X} = 0.0$ and $\overline{X} = 0.128$. With this type of *marching* solution one is not able to observe the variations of the velocity field with successive iterations. Therefore, we had to resort to the relative error as a measure of convergence. This was done by setting successively smaller tolerances on the relative error until the computed results were no longer dependent on the relative error required for convergence.

The centerline velocities for the boundary-layer solution and the complete solution are shown in Figure 10. Although it is not necessary that the solution of Equations (4) and (5) become identical with the boundary-layer solution as $N_{Re} \to \infty$, one would expect that the boundary-layer solution would provide an upper bound for the set of increasing Reynolds numbers, but this is not the case for values of $\overline{X}$ greater than 0.001. The boundary-layer results shown in Figure 10 were obtained for $\Delta Y = 0.05$ and $\Delta\overline{X} = 2^{i-1}\,(0.00025)$, where i is the number of steps taken in the $\overline{X}$ direction. Additional results were obtained for (1) $\Delta Y = 0.025$ and $\Delta\overline{X} = 2^{i-1}\,(0.00025)$, and (2) $\Delta Y = 0.05$ and $\Delta\overline{X} = 1.5^{i-1}\,(0.000125)$ which showed no effect of mesh size on the computed results.

The boundary conditions for the boundary-layer equations are

$$\text{B.C. } 4a \quad \psi = \Omega = 0,\ Y = 0 \tag{51}$$

$$\text{B.C. } 2b \quad \psi = 2/3,\ \frac{\partial^2\Omega}{\partial Y^2} = 0,\ Y = 1 \tag{52}$$

Imposition of the boundary condition for the vorticity at $Y = 1$ is not a straightforward operation, since all the terms in the differential equation tend to zero as $Y \to 1$. An attempt was made to impose this condition by writing

$$\Omega^{k+1}{}_{n,J} - 2\widetilde{\Omega}^{k}{}_{n,J-1} + \widetilde{\Omega}^{k}{}_{n,J-2} = 0 \tag{53}$$

If the solution converged, it would have to satisfy B.C. 2*b*, since convergence requires $\Omega^{k+1}{}_{n,j} = \widetilde{\Omega}^{k}{}_{n,j}$; however, the iterative procedure did not converge when the boundary condition was formulated in this manner. Jenson's method (4), which makes use of Equation (42) subject to the restriction $\frac{\partial\psi}{\partial Y} = 0$ at $Y = 1$, did work satisfactorily for this case. Churchill (4) also has indicated that direct numerical solution of the vorticity equation on solid boundaries leads to instability at high Reynolds numbers, and Jenson's method must be used. The reasonable agreement between the complete solution and the boundary-layer solution, both for the centerline velocities and the velocity profiles shown in Figure 11, indicates that either method of specifying the vorticity boundary condition is satisfactory.

MACROSCOPIC MOMENTUM BALANCE

For the boundary-layer solution and the higher Reynolds numbers for the complete solution, a macroscopic momentum balance can provide some indication of the

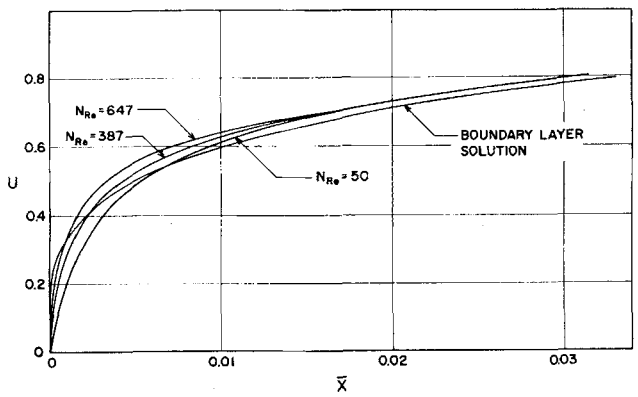

Fig. 10. Centerline velocity.

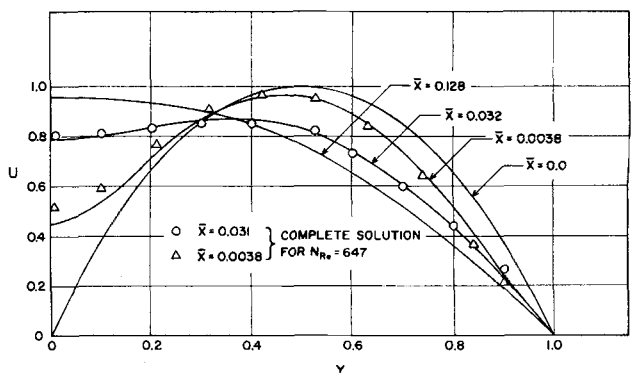

Fig. 11. Velocity profiles for boundary-layer solution.

accuracy of the results. The momentum balance may be written as

$$\left\{\begin{matrix}\text{momentum flux}\\ \text{out}\end{matrix}\right\}-\left\{\begin{matrix}\text{momentum flux}\\ \text{in}\end{matrix}\right\}=\left\{\begin{matrix}\text{pressure}\\ \text{force}\end{matrix}\right\}+\left\{\begin{matrix}\text{surface}\\ \text{force}\end{matrix}\right\} \quad (54)$$

$$\left\{\begin{matrix}\text{momentum}\\ \text{flux}\\ \text{out}\end{matrix}\right\}=\int_o^1 U^2_X dY$$

$$\left\{\begin{matrix}\text{momentum}\\ \text{flux}\\ \text{in}\end{matrix}\right\}=\int_o^1 U^2_o dY$$

$$\left\{\begin{matrix}\text{pressure}\\ \text{force}\end{matrix}\right\}=-\int_o^X \frac{\partial \bar{P}}{\partial X} dX$$

$$\left\{\begin{matrix}\text{surface}\\ \text{force}\end{matrix}\right\}=-\frac{1}{N_{Re}}\int_o^X \left(\frac{\partial U}{\partial Y}\right) dX \Bigg|_{Y=0}+\frac{1}{N_{Re}}\int_o^X \left(\frac{\partial U}{\partial Y}\right) dX \Bigg|_{Y=1}$$

where

$$\frac{\partial \bar{P}}{\partial X}=\frac{1}{N_{Re}}\int_v^1 \left(\frac{\partial^2 U}{\partial X^2}+\frac{\partial^2 U}{\partial Y^2}\right) dY - \int_o^1 \left(U\frac{\partial U}{\partial X}+V\frac{\partial U}{\partial Y}\right) dY$$

Substitution of the appropriate terms into Equation (54) plus some simple algebraic manipulation yields

$$\int_o^1 U^2_X dY - 2\int_o^X \int_o^1 V\frac{\partial U}{\partial Y} dY\, dX - \int_o^1 U^2_o dY = 0 \quad (55)$$

Thus we see that the pressure and surface forces are identical except for the double integral in Equation (55). The percentage error, shown in Figure 12 for the boundary-layer solution and $N_{Re} = 647$, is defined as

Percentage error

$$= \left\{1 - \frac{\int_o^1 U^2_X dY - 2\int_o^X \int_o^1 V\frac{\partial U}{\partial Y} dY\, dX}{\int_o^1 U^2_o dY}\right\} \times 100 \quad (56)$$

The results shown in Figure 12 indicate that the error in the macroscopic momentum balance is quite small, and cannot explain the unexpected results shown in Figure 10. In addition, the macroscopic material balance for these two cases shows negligible error.

It seems quite reasonable that Equations (43) to (45) or the equivalent, Equations (41) and (42), are capable of providing satisfactory results for high Reynolds number. The numerical solution of these boundary-layer equations should be accurate, since both the effect of mesh size and of convergence tolerance on the computed velocity profiles were carefully examined. Differences between the complete solution at high Reynolds numbers and the boundary-layer solution may result from one or all of the following causes. (1) The Reynolds number must be larger than 647 in order that the boundary-layer equations become satisfactory. (2) Imposition of the downstream boundary condition at some finite value of X may have caused more error than is indicated in Figure 4. (3) The mesh size for the complete solution may not have been small enough. In any event, the differences between the two solutions are not large, and both satisfy the macroscopic momentum balance quite closely.

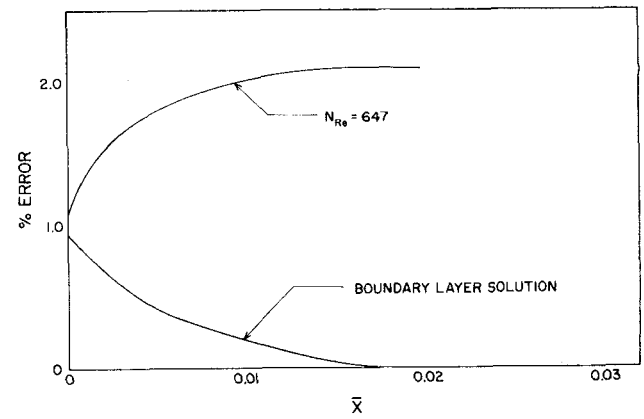

Fig. 12. Error for macroscopic momentum balance.

CONCLUSIONS

The methods presented for solving both the complete equations of motion and a set of boundary-layer equations for incompressible, isothermal, Newtonian fluids appear to provide a satisfactory route to investigate flows of this type over the entire range of Reynolds numbers for which steady flows can be expected. Application of these techniques to practical problems should be accompanied by a more thorough investigation of the error than was presented here. An examination of the effect of the mesh size and the location of boundary conditions should be carried out in every case.

NOTATION

h = channel depth for $x < o$, cm.
$J+1$ = number of points in the y direction for the finite-difference network
k = number of iterations
$N+1$ = number of points in the x direction for the finite-difference network
N_{Re} = $u_m h/\nu$
p = fluid pressure, dyne/sq. cm.
P = $p/\rho u_m^2$, dimensionless fluid pressure
u,v = scalar components of the velocity vector in the x and y directions, respectively, cm./sec.
U,V = u/u_m, v/u_m, dimensionless velocity components
x,y = rectangular Cartesian coordinates, cm.
X,Y = x/h, y/h, dimensionless coordinates
X_{max} = location of downstream boundary condition
$\bar{X}$ = X/N_{Re}
u_m = centerline velocity at $x = \infty$, cm./sec.

Greek Letters

α = iteration parameter, dimensionless
ρ = fluid density, g./cc.
ψ = dimensionless stream function
Ω = dimensionless vorticity

Subscripts

j,n = points on the finite-difference network where $X_n = n\Delta X$ and $Y_j = j\Delta Y$
o = function is evaluated at $X = 0$
X = function is evaluated at X

Superscripts

i = number of steps in the $\bar{X}$ direction
k = the value for the k^{th} iteration
$\sim$ = an assumed value based on a previous calculation

LITERATURE CITED

1. Allen, D. N. deG., and R. V. Southwell, *Quart. J. Mech. Appl. Math.*, **8**, 129 (1955).
2. Beutler, J. A., Jr., personal communication (1961).
3. Birkhoff, Garrett, "Hydrodynamics—A Study in Logic, Fact and Similitude," Princeton Univ. Press, Princeton, N. J. (1960).
4. Churchill, S. W., personal communication (1965).
5. Flumerfelt, R. W., and J. C. Slattery, *Chem. Eng. Sci.*, **20**, 157 (1965).
6. Hausen, A. G., *Trans. Am. Soc. Mech. Engrs.*, **80**, 1553 (1958).
7. ———, "Similarity Analysis of Boundary Value Problems in Engineering," Prentice-Hall, Englewood Cliffs, N. J. (1964).
8. Jenson, V. G., *Proc. Roy. Soc. (London)*, **A249**, 346 (1959).
9. Kawaguti, Mitutosi, *J. Phys. Soc. Jap.*, **10**, 695 (1955).
10. *Ibid.*, **8**, 747 (1953).
11. Kuwabara, Shinji, *J. Phys. Soc. Jap.*, **13**, 1516 (1958).
12. Michal, A. D., *Proc. Natl. Acad. Sci. (U.S.)*, **37**, 623 (1951).
13. Morse, P. M., and Herman Feshbach, "Methods of Theoretical Physics," McGraw-Hill, New York (1953).
14. Paris, Jean, M.S. thesis, Northwestern Univ., Evanston, Ill. (1963).
15. Peaceman, D. W., G. H. Bruce, and H. H. Rachford, *Trans. Am. Soc. Mech. Engrs.*, **198**, 79 (1953).
16. Schlichting, Hermann, "Boundary Layer Theory," McGraw-Hill, New York (1955).
17. Slattery, J. C., *Chem. Eng. Sci.*, **19**, 801 (1964).
18. Southwell, R. V., "Relaxation Methods in Theoretical Physics," Clarendon Press, Oxford (1946).
19. Snyder, L. J., and W. E. Stewart, paper presented at A.I.Ch.E. Houston meeting (February, 1965).
20. Snyder, L. J., T. W. Spriggs, and W. E. Stewart, *A.I.Ch.E. J.*, **10**, 535 (1964).
21. Thom, A., *Proc. Roy. Soc. (London)*, **A141**, 651 (1933).
22. ———, and C. J. Opelt, "Field Computation in Engineering and Physics," Van Nostrand, London (1961).
23. Thomas, L. H., unpublished information, see reference *15*.
24. Wang, Y. L., and P. A. Longwell, *A.I.Ch.E. J.*, **10**, 323 (1964).
25. Wendel, M. M., personal communication (1961).
26. ———, and Stephen Whitaker, *Appl. Sci. Res.*, **A12**, 91 (1963).
27. *Ibid.*, 313.
28. Young, David, and Louis Ehrlich, "Boundary Problems in Differential Equations," R. E. Langer, ed., Univ. Wisconsin Press, Madison (1960).
29. Fromm, J. E., and F. H. Harlow, *Phys. Fluids*, **6**, 975 (1963).
30. Pearson, C. E., *J. Fluid Mech.*, **21**, 611 (1965).
31. Peaceman, D. W., and H. H. Rachford, *J. Soc. Ind. Appl. Math.*, **3**, 28 (1965).

Manuscript received March 22, 1965; revision received July 12, 1965; paper accepted July 26, 1965. Paper presented at A.I.Ch.E. Houston meeting.

Analysis and Design of Gas Flow Reactors with Applications to Hydrocarbon Pyrolysis

MICHAEL L. TROMBETTA and JOHN HAPPEL

New York University, New York, New York

The analysis and design of gas flow reactors are customarily based on a plug flow model. Because of transverse concentration and temperature gradients, however, kinetic constants and reactor lengths based on the plug flow model may be in gross error. This paper presents an approximate method of analysis which accounts for the effects of these gradients. We examine a gas in laminar flow which supports a first-order irreversible reaction. Compressibility effects are considered, and the diffusion fluxes are calculated with the full ternary diffusion equations. Instead of solving exactly the full equations of change which describe this system, the well-known Pohlhausen technique is adapted and approximate solutions which satisfy the integral forms of these equations are sought. This reduces the problem to the solution of a set of ordinary differential equations, which are integrated numerically. The main result is a set of graphs giving correction factors to be applied to plug flow kinetic constants and reactor lengths. Although primary interest is in hydrocarbon pyrolysis systems, the integral method graphs are applicable to other reaction systems.

Chemical engineers are often called upon to solve the two closely related problems: (1) Given conversion data obtained in a gas flow reactor, analyze the data to determine reaction rate constant. (2) Given reaction rate constants, design a gas flow reactor to obtain a specified conversion. We may call these, respectively, the analysis and design problems.

Michael L. Trombetta is with Shell Chemical Company, New York, New York.

Hougen and Watson (*1*) presented solutions to these problems which were based on the assumption that the concentration profile was flat, the plug flow or one-dimensional model. Cleland and Wilhelm (*2*) considered the effect of a radial concentration gradient on a first-order reaction in an incompressible, isothermal fluid. The conservation equation for the reactant was integrated numerically. Later, Lauwerier (*3*) solved this problem analytically in terms of an infinite series of eigenfunctions.